

Inverse energy transfer in finite-temperature superfluid vortex reconnections

P. Z. Stasiak, A. Baggaley, and C.F. Barenghi
*School of Mathematics, Statistics and Physics, Newcastle University,
Newcastle upon Tyne, NE1 7RU, United Kingdom*

G. Krstulovic
*Université Côte d’Azur, Observatoire de la Côte d’Azur, CNRS, Laboratoire Lagrange,
Boulevard de l’Observatoire CS 34229 - F 06304 NICE Cedex 4, France*

L. Galantucci
*Istituto per le Applicazioni del Calcolo “M. Picone” IAC CNR, Via dei Taurini 19, 00185 Roma, Italy
(Dated: February 4, 2025)*

Vortex reconnections play a fundamental role in fluids and they are typically considered as a mechanism to increase their complexity and to develop small scales. In this work, we show that in superfluids, they can also create large scale structures. We numerically show that during a superfluid vortex reconnection energy is injected into the thermal (normal) component of helium II at small length scales, but is transferred nonlinearly to larger length scales, increasing the integral length scale of the normal fluid. We provide an explanation of this inverse energy transfer by decomposing the velocity and the mutual friction (which couples superfluid and normal fluid) into helical modes, showing that the imbalance of homochiral modes results from the punctuated energy and helicity injection during the reconnection. Finally, we discuss the relevance of our findings to the problem of superfluid turbulence.

Turbulence is ubiquitous in the universe. It occurs in systems as large as nebulae of interstellar gas, and as small as clouds of few thousands atoms confined by lasers in the laboratory. Turbulence shapes patterns and properties of fluids of all kinds, from ordinary viscous fluids (Navier-Stokes turbulence [1]) to electrically conducting fluids (magneto-hydrodynamics turbulence [2]) to quantum fluid (quantum turbulence [3, 4]). All turbulent systems are characterised by the existence of a wide range of length scales across which inviscid conserved quantities are transferred without loss in the spirit of the cascade depicted by Richardson [5].

In three-dimensional classical fluids, turbulence is characterised by a direct cascade: the non-linear dissipationless transfer of kinetic energy from the scale of the large eddies (at which energy is injected) to the smallest length scales at which energy is dissipated into heat [5, 6]. The resulting distribution of energy across length scales is the celebrated Kolmogorov energy spectrum [1, 6].

Confining Navier-Stokes turbulence to two-dimensions entails fundamentally distinct physics: a dual cascade emerges of energy and enstrophy (mean squared vorticity) [7, 8], the two conserved quantities in ideal two-dimensional flows. In particular, while the enstrophy cascade is direct (from large to small scales), the energy cascade is inverse (from small to large scales) [9]. This inverse cascade may favour the generation and persistence of large coherent structures [10].

Remarkably, the same cascade phenomenology is observed in turbulent flows of quantum fluids, *i.e.* fluids at very low temperatures whose physics is dominated by quantum effects. Examples of such fluids are superfluid

helium and atomic Bose-Einstein Condensates (BECs). The dynamics of these systems can be successfully depicted in terms of a two-fluid model [11–13] describing the quantum fluid as the mixture of two components, the superfluid component and the thermal (or normal) component, which interact by means of a mutual friction force [14–16]. The superfluid component flows without viscosity and vanishing entropy; its vorticity is confined to effectively one-dimensional vortex filaments of atomic core thickness (called quantum vortices or vortex lines), around which the circulation of the velocity is quantised. In BECs the thermal component forms a ballistic gas, whereas in superfluid ^4He it can be described as a classical viscous fluid. Despite these significant differences with respect to ordinary fluids, the forward kinetic energy cascade has indeed been observed in three-dimensional superfluid turbulence [17–22]. Evidence of this forward cascade has been found also in three-dimensional turbulent BECs [23]. Similarly to 2D classical turbulence, an inverse energy cascade characterises two-dimensional BECs, as shown in theoretical [24–27] and experimental [28, 29] studies.

In turbulent systems, the type and the number of sign-defined ideal invariants determine the direction of cascades. Indeed, the famous and simple Fjørtoft argument [30] predicts in 2D classical turbulence the existence of an inverse energy cascade. Similarly, for 3D wave-turbulent 3D BECs, the Fjørtoft argument predicts an inverse particle and a direct energy cascade, as recently addressed theoretically [31]. In 3D classical fluids, helicity, which is also an inviscid invariant, is not sign-defined and thus only a direct energy cascade is possible. However, re-

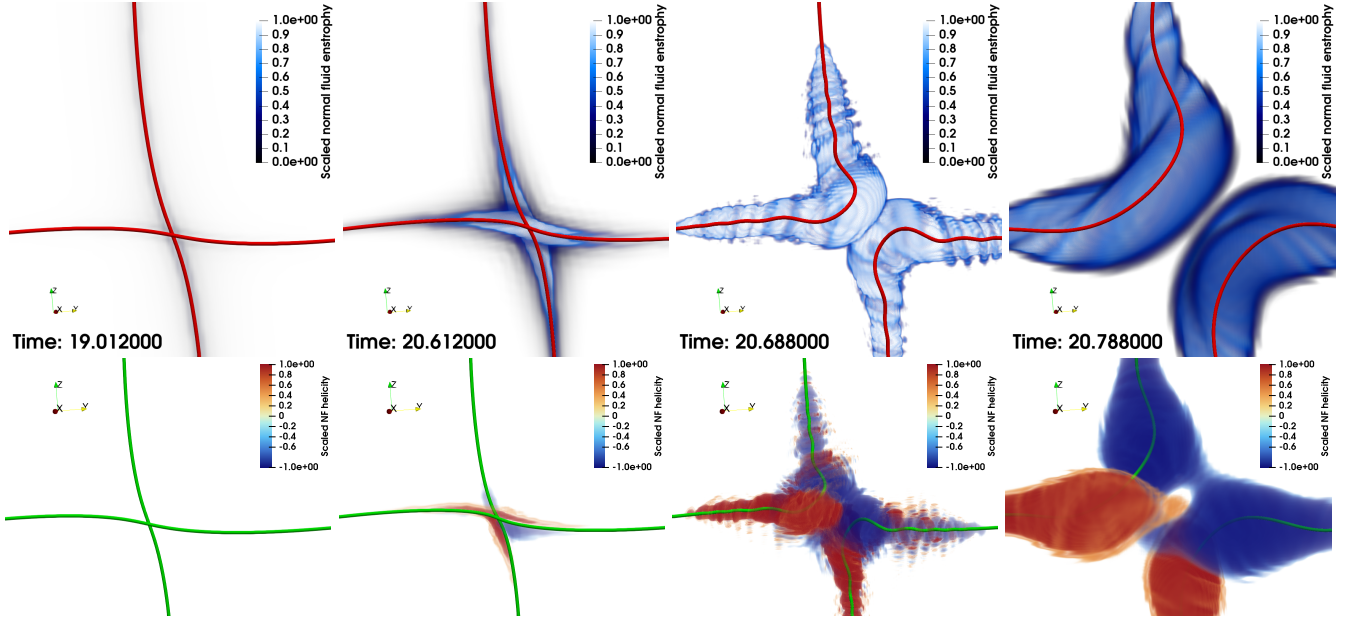


FIG. 1: Three-dimensional rendering of an orthogonal vortex configuration undergoing a vortex reconnection. The red tubes represent the superfluid vortex lines (the tubes' radii have been greatly exaggerated for visual purposes), and the blue volume rendering represents the scaled normal fluid enstrophy ω^2/ω_{max}^2 . In the third panel, note the Kelvin waves on the superfluid vortices. [$T=?$] **[GK: update caption once we decided if we keep both rows. How is helicity scaled?]**

cent studies have demonstrated that the direction of the energy cascade may be inverted by artificially controlling the chirality of the flow, *i.e.* the balance between positive or negative helical modes [32], eventually making helicity almost a sign defined quantity. Indeed, by restricting the non-linear energy transfer to homochiral interactions via a suitable decimation of the Navier-Stokes equation [33, 34], controlling the weight of homochiral interactions [35] or the external injection of positive helical modes at all length scales [36], inverse energy cascades have been observed in three-dimensional turbulence of classical fluids. In brief, when the flow is synthetically designed to have an enhanced chirality, an inverse energy cascade can be observed.

In this work, we unveil a similar dynamics occurring in superfluid helium (^4He) as a result of vortex reconnections. Reconnections occur continuously in turbulence: they take place when two vortex lines collide and recombine, exchanging heads and tails, altering the overall topology of the flow [37–43]. We show that the mutual friction force arising from the vortex reconnection is chiral, injecting in the normal fluid prevalently helicity of a given sign. Thus, as a consequence of vortex reconnections, we observe an increase of the chiral imbalance of the quantum fluid, producing a transfer of kinetic energy from small to large scales, similarly to the phenomenology observed in 3D helical-decimated classical flows. Unlike classical fluids, such a chiral imbalance arises naturally as physical process in the normal fluid.

To model superfluid helium dynamics, we employ the recently developed FOUCAULT model [44]. In this approach, superfluid vortex lines are parametrized as one-dimensional space curves $\mathbf{s}(\xi, t)$, ξ and t being arclength and time respectively, exploiting the large separation of length scales between the vortex core radius, the Lagrangian discretisation along the vortex lines $\Delta\xi$, and the average radius of curvature R_c of the vortex lines. The vortex lines evolve according to the following equation of motion:

$$\dot{\mathbf{s}}(\xi, t) = \mathbf{v}_s + \frac{\beta}{1 + \beta} [\mathbf{v}_{ns} \cdot \mathbf{s}'] \mathbf{s}' + \beta \mathbf{s}' \times \mathbf{v}_{ns} + \beta' \mathbf{s}' \times [\mathbf{s}' \times \mathbf{v}_{ns}], \quad (1)$$

where $\dot{\mathbf{s}} = \partial\mathbf{s}/\partial t$, $\mathbf{s}' = \partial\mathbf{s}/\partial\xi$ is the unit tangent vector, \mathbf{v}_n and \mathbf{v}_s are the normal fluid and superfluid velocities at \mathbf{s} , $\mathbf{v}_{ns} = \mathbf{v}_n - \mathbf{v}_s$, and β, β' are temperature and Reynolds number dependent mutual friction coefficients [44]. The calculation of the superfluid velocity \mathbf{v}_s is performed via the computation of the Biot-Savart integral de-singularised with standard techniques (see Supplementary Material [45]). The normal fluid is described classically using the incompressible ($\nabla \cdot \mathbf{v}_n = 0$) Navier-Stokes equation

$$\frac{\partial \mathbf{v}_n}{\partial t} + (\mathbf{v}_n \cdot \nabla) \mathbf{v}_n = -\frac{1}{\rho} \nabla p + \nu_n \nabla^2 \mathbf{v}_n + \frac{\mathbf{F}_{ns}}{\rho_n}, \quad (2)$$

where ρ_n and ρ_s are the normal fluid and superfluid densities, $\rho = \rho_n + \rho_s$, p is the pressure, ν_n is the kinematic viscosity of the normal fluid, and the mutual friction force

per unit volume, \mathbf{F}_{ns} , is the line integral of the mutual friction force per unit length, \mathbf{f}_{ns} [45]:

$$\mathbf{F}_{ns}(\mathbf{x}) = \oint_C \delta(\mathbf{x} - \mathbf{s}) \mathbf{f}_{ns}(\mathbf{s}) d\xi, \quad (3)$$

\mathcal{C} representing the entire vortex configuration. The regularisation of mutual friction is performed using a physically self-consistent scheme [44]. We consider a periodical box of size 2π (so that wavevectors are integers).

To study the reconnection dynamics, we consider two pairs of initially orthogonal vortices (where the corresponding vortices of each pair have opposite circulation in order to preserve periodicity along the boundaries) at two temperatures, $T = 1.9K$ and $T = 2.1K$. The vortex pairs are separated by the distance D_ℓ ; each vortex within each pair is initially at distance d_ℓ to the other vortex, such that $d_\ell \ll D_\ell$ to ensure that the dynamics in the vicinity of the reconnection is dominated by local interactions, and that the far-field contribution from the other vortex pair is negligible.

The evolution of the vortex reconnection of a single pair is reported in Fig. 1. The first row shows the reconnecting superfluid vortices (in red) accompanied by normal fluid structures generated by mutual friction, here displayed as enstrophy rendering $\omega(\mathbf{x})^2 = |\nabla \times \mathbf{v}_n|^2$. Such structures are the signature of the violent irreversible energy transfers in vortex reconnections reported in [46] **[GK:remove this sentence if we delete the first row of the figure]**. The second row shows the rendering of the local helicity $H(\mathbf{x}) = \mathbf{v}_n \cdot (\nabla \times \mathbf{v}_n)$, where we observe a clear local helicity production, with an abrupt change of sign due to the rearrangement of the vortex topology. Remarkably, during reconnection there is a net normal fluid helicity production, as shown in Fig. 2. We will come back to this finding later. **[GK: update text depending on the final figure.]**

We now focus on the time evolution of the normal fluid energy spectrum $E(k)$ (where k is the magnitude of the three-dimensional wavenumber), displayed in Fig. 3.a. It clearly emerges that, during the reconnection, energy is predominantly injected into the normal fluid at intermediate and small length scales. For $k > 5$ in correspondence of the reconnection time t_0 , we observe a significant increase of the normal fluid energy spectral density: $E(k, t \approx t_0)/E(k, t \ll t_0) \approx 10^2$.

In the post-reconnection regime, we simultaneously observe a small decrease of the spectrum at intermediate and small scales ($k > 5$) and an increase at large scales, suggesting the existence of a mechanism by which energy generated at small length scales is transferred to larger scales. To shed light on this mechanism we analyse the dynamics of the normal fluid flow using the spectral energy budget equation:

$$\frac{\partial E(k)}{\partial t} = T(k) - D(k) + I(k) \quad (4)$$

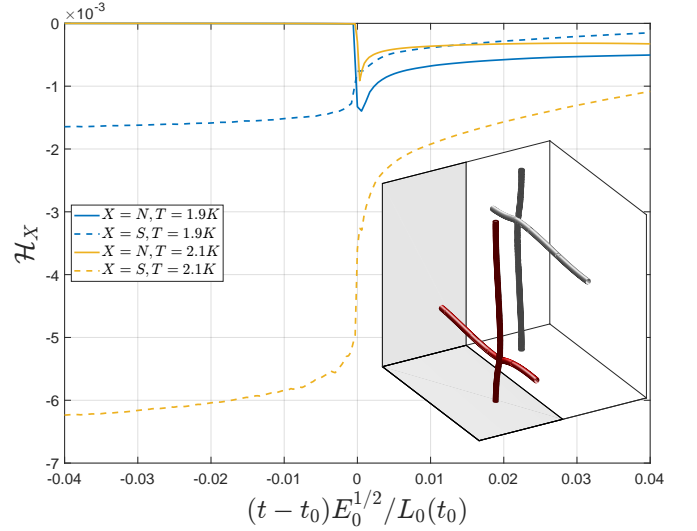


FIG. 2: Temporal evolution of the normal fluid helicity computed over half of the box to consider only one pair of vortices (gray zone). *Inset*: Whole computational box showing the two pairs of vortices. **[change for just the total helicity]**

where $T(k)$ is the spectral kinetic energy transfer function, $D(k) = 2\nu_n k^2 E_k$ is the dissipation spectrum and $I(k)$ is the injection spectrum arising from the mutual friction force \mathbf{F}_{ns} . Immediately after the reconnection, each vortex has the shape of a sharp cusp (corresponding to a small radius of curvature R_c) which immediately starts relaxing (R_c increases). Since $|\mathbf{F}_{ns}| \propto |\dot{\mathbf{s}} - \mathbf{v}_n| \approx |\dot{\mathbf{s}}| \propto 1/R_c$, the scales of energy injection at reconnection are necessarily much smaller than the original length scales before the reconnection, as it can be observed in Fig. 3.b As time evolves, the smallest perturbations on the vortex lines are damped by friction the fastest, resulting in the shift of the peak of the injection spectrum $I(k)$ towards larger length scales. However this shift does not account for the increase of $E(k)$ at the largest scales after reconnection, which arises from non-linear effects. Indeed, if we compute the energy flux $\Pi(k) = \int_k^\infty T(k') dk'$ (reported in Fig. 4 at different times and temperatures), we observe that $\Pi(k) < 0$ for all k during and after reconnection; we also observe that, near the time of reconnection, the peak value of $|\Pi(k)|$ is in the range $5 < k < 15$. The negative sign of $\Pi(k)$ is evidence of a flux of kinetic energy from small to large scales. In other words, at non-zero temperatures, vortex reconnections trigger an inverse transfer of energy, which implies the creation of large scale structures, visible in Fig. 1 **[GK: the figure shows small scale structures...]** This effect is quantified by the evolution of the integral length scale L_0 ,

defined as

$$L_0 = \frac{\pi}{2K} \int_0^\infty \frac{E(k)}{k} dk / \int_0^\infty E(k) dk. \quad (5)$$

The inset of Fig. 4 shows that L_0 indeed increases steadily in the post-reconnection regime. Note that times have been normalised by the largest eddy-turnover-time at the reconnection event, evidencing its quick evolution.

To explain the inverse energy transfer shown in Fig. 3, we look whether the reconnection triggers a chirality imbalance. We decompose the incompressible Fourier modes of the normal fluid velocity into helical modes [47]:

$$\hat{\mathbf{v}}_n(\mathbf{k}) = \hat{\mathbf{v}}_n^+(\mathbf{k}) + \hat{\mathbf{v}}_n^-(\mathbf{k}) = v_n^+(\mathbf{k})\mathbf{h}^+(\mathbf{k}) + v_n^-(\mathbf{k})\mathbf{h}^-(\mathbf{k}), \quad (6)$$

where $\mathbf{h}^\pm(\mathbf{k})$ are the two eigenvectors of the curl operator, *i.e.* $i\mathbf{k} \times \mathbf{h}^\pm(\mathbf{k}) = \pm k\mathbf{h}^\pm(\mathbf{k})$. Similarly, we

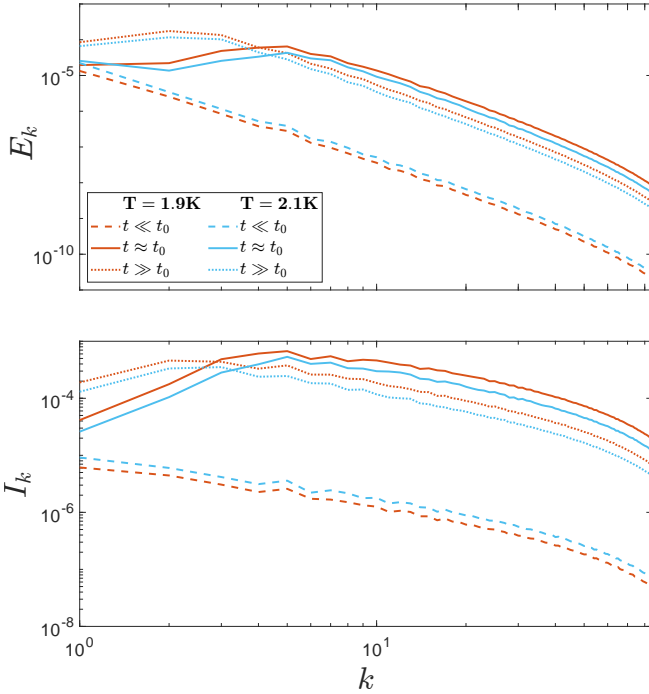


FIG. 3: a) Normal fluid kinetic energy spectrum $E(k)$ before reconnection (dashed lines), at reconnection (solid lines) and after reconnection (dotted lines) for $T = 1.9K$ (red) and $T = 2.1K$ (blue). b) Energy injection spectrum $I(k)$ arising from the mutual friction forcing at the same times as in the main figure. **[GK:**

I'm not sure that we really need the the injection spectrum, it doesn't have a clear peak and it is very similar to $E(k)$. If we remove, we could simplify the text where we talk about the spectral energy budget that we do not really use (we don't show the dissipation, and we won't do it neither). If we manage to have some visualisation of the large scales, it could replace this figure...]

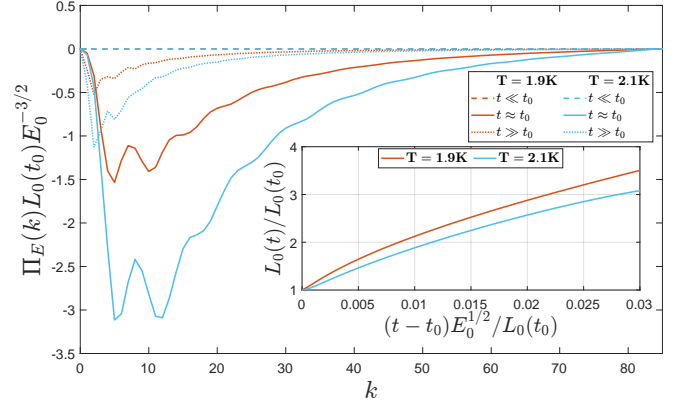


FIG. 4: *Top*: Mutual friction injection spectrum, I_k . *Bottom*: Spectral normal fluid kinetic energy flux, Π_E . It is normalised by using the integral scale and the normal fluid energy at reconnection. *Inset*: Post reconnection evolution of the integral length scale, L_0 . Times and temperatures are labelled as in Fig. 3

decompose the Fourier of the transverse mutual friction force: $\mathbf{F}_{ns}^\perp(\mathbf{k}) = f^+(\mathbf{k})\mathbf{h}^+ + f^-(\mathbf{k})\mathbf{h}^-$ (the Fourier modes of \mathbf{F}_{ns} parallel to the wavenumber \mathbf{k} do not play any role in the time evolution of \mathbf{v}_n due to the incompressible constraint). The spectral energy densities corresponding to the helical modes are $E^\pm(\mathbf{k}) = (1/2)|v_n^\pm(\mathbf{k})|^2$, the total spectral density being $E(\mathbf{k}) = E^+(\mathbf{k}) + E^-(\mathbf{k})$. Similarly the spectral helicity density is

$$H(\mathbf{k}) = (1/2)\hat{\mathbf{v}}_n(\mathbf{k}) \cdot \hat{\boldsymbol{\omega}}_n^*(\mathbf{k}) = kE^+(\mathbf{k}) - kE^-(\mathbf{k}) = H^+(\mathbf{k}) - H^-(\mathbf{k}), \quad (7)$$

where $\boldsymbol{\omega}_n$ is the normal fluid vorticity, the star indicates complex conjugate and H^\pm is the helicity contribution of each separate helical mode. **[GK: the standard definition of the energy and helicity spectra contains the sum over the angles, so the previous definition are wrong (except if you redefined them for some reason).]**

A chiral imbalance occurs if the mutual friction force is helical, *i.e.* if the ratio $|f^+|^2/|f^-|^2 \neq 1$, with $|f^\pm|^2$ the total squared norm the component. In Fig. 5, we show the temporal evolution of $|f^+|^2/|f^-|^2$, for both temperatures. It is apparent that during and after the reconnection, the mutual friction force is chiral, injecting more negative helicity than positive helicity. As a result, the ratio $\mathcal{H}^+/\mathcal{H}^-$ (reported in the inset of Fig. 5), where $\mathcal{H}^\pm(t) = \int H^\pm(\mathbf{k}, t) d\mathbf{k}$ **[GK: this one is consistent with the definition]**, decreases significantly at reconnection and remains smaller than unity even at later times, indicating that the flow is chiral. We conclude that the reconnection triggers indeed a chiral imbalance.

In conclusion, the reconnection of quantum vortices in the two-fluid regime ($T \gtrsim 1.5K$) not only injects punctuated energy in the normal fluid [46], but also triggers in

the normal fluid a transfer of kinetic energy towards the large scales. This inverse energy transfer arises from the fact that the mutual friction force (injecting energy and helicity in the normal fluid) is helical, as Kelvin waves develop on the vortices. The helical character of the mutual friction produces a chiral imbalance in the normal fluid, driving this inverse cascade as previously observed in turbulent Navier-Stokes flows [33, 36]. Our findings have profound implications **[GK: which ones?]** for the nature of finite temperature superfluid turbulence and motivate a detailed studied of fully coupled quantum turbulence to understand how energy transfer and dissipation is augmented by vortex reconnections.

[Can a flow sustain a constant injection with multiple reconnections? Maybe by ring injection? From last peter's plots, the injection last for about $\kappa.1$ (and much less the strong imbalance). How is this time compared with typical reconnection time in experiments? What would be the ultimate turbulent state/spectrum?]

G.K. was supported by the Agence Nationale de la Recherche through the project the project QuantumVIW ANR-23-CE30-0024-02. This work has been also supported by the French government, through the UCAJEDI Investments in the Future project managed by the National Research Agency (ANR) with the reference number ANR-15-IDEX-01. P.Z.S. acknowledges the financial support of the UniCA “visiting doctoral student program” on complex systems. Computations were carried out at the Mésocentre SIGAMM hosted at the Observatoire de la Côte d’Azur **[GK: true?]**.

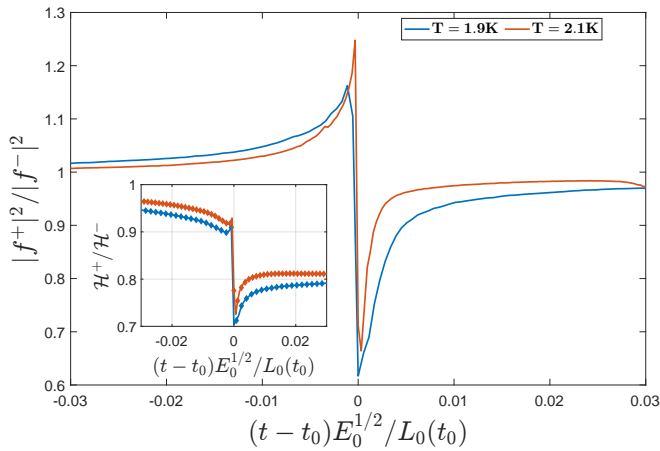


FIG. 5: Temporal evolution of projected mutual friction force components $f^\pm/|f^\pm|^2$. Inset: temporal evolution of total helical components.

- [1] U. Frisch, *Turbulence: The Legacy of A. N. Kolmogorov* (1995).
- [2] V. M. Canuto and J. Christensen-Dalsgaard, Turbulence in astrophysics: stars, *Ann. Rev. Fluid Mech.* **30**, 167 (1998).
- [3] C. F. Barenghi, H. A. J. Middleton-Spencer, L. Galantucci, and N. G. Parker, Types of quantum turbulence, *AVS Quantum Sci.* **5**, 025601 (2023).
- [4] C. F. Barenghi, L. Skrbek, and K. R. Sreenivasan, *Quantum Turbulence* (Cambridge University Press, 2023).
- [5] L. F. Richardson, *Weather Prediction by Numerical Process* (University Press, 1922).
- [6] A. Kolmogorov, The local structure of turbulence in an incompressible viscous fluid for very large Reynolds numbers, *Dokl. Akad. Nauk. SSSR* **30**, 301 (1941).
- [7] R. Kraichnan, Inertial ranges in two-dimensional turbulence, *Phys. Fluids* **10**, 1417 (1967).
- [8] G. Boffetta and R. E. Ecke, Two-dimensional turbulence, *Ann. Rev. Fluid Mech.* **44**, 427 (2012).
- [9] G. Boffetta and S. Musacchio, Evidence for the double cascade scenario in two-dimensional turbulence, *Phys. Rev. E* **82**, 016307 (2010).
- [10] J. Laurie, G. Boffetta, G. Falkovich, I. Kolokolov, and V. Lebedev, Universal profile of the vortex condensate in two-dimensional turbulence, *Phys. Rev. Lett.* **113**, 254503 (2014).
- [11] L. Tisza, Transport phenomena in helium II, *Nature* **141**, 913 (1938).
- [12] L. Landau, On the theory of superfluidity, *Phys. Rev.* **75**, 884 (1949).
- [13] L. Skrbek and K. R. Sreenivasan, Developed quantum turbulence and its decay, *Phys. Fluids* **24**, 011301 (2012).
- [14] B. Jackson, N. P. Proukakis, C. F. Barenghi, and E. Zaremba, Finite-temperature vortex dynamics in bose-einstein condensates, *Phys. Rev. A* **79**, 053615 (2009).
- [15] H. E. Hall and W. F. Vinen, The rotation of liquid helium II. i. experiments on the propagation of second sound in uniformly rotating helium II, *Proc. R. Soc. London A* **238**, 204 (1956).
- [16] H. E. Hall and W. F. Vinen, The rotation of liquid helium II. ii. the theory of mutual friction in uniformly rotating helium II, *Proc. R. Soc. London A* **238**, 215 (1956).
- [17] J. Maurer and P. Tabeling, Local investigation of superfluid turbulence, *Europhys. Lett.* **43**, 29 (1998).
- [18] J. Salort, C. Baudet, B. Castaing, B. Chabaud, F. Daviaud, T. Didelot, P. Diribarne, B. Dubrulle, Y. Gagne, F. Gauthier, A. Girard, B. Hébral, R. B., P. Thibault, and P.-E. Roche, Turbulent velocity spectra in superfluid flows, *Phys. Fluids* **22** (2010).
- [19] A. W. Baggaley, L. K. Sherwin, C. F. Barenghi, and Y. A. Sergeev, Thermally and mechanically driven quantum turbulence in helium II, *Phys. Rev. B* **86**, 104501 (2012).
- [20] L. K. Sherwin-Robson, C. F. Barenghi, and A. W. Baggaley, Local and nonlocal dynamics in superfluid turbulence, *Phys. Rev. B* **91**, 104517 (2015).
- [21] N. P. Müller and G. Krstulovic, Kolmogorov and Kelvin wave cascades in a generalized model for quantum turbulence, *Physical Review B* **102**, 134513 (2020).
- [22] N. P. Müller, J. I. Polanco, and G. Krstulovic, Intermittency of Velocity Circulation in Quantum Turbulence,

- Physical Review X **11**, 011053 (2021).
- [23] H. A. J. Middleton-Spencer, A. D. G. Orozco, L. Galantucci, M. Moreno, N. G. Parker, L. A. Machado, V. S. Bagnato, and C. F. Barenghi, Evidence of strong quantum turbulence in Bose-Einstein condensates, *Phys. Rev. Research* **5**, 043081 (2022).
 - [24] A. S. Bradley and B. P. Anderson, Energy spectra of vortex distributions in two-dimensional quantum turbulence, *Phys. Rev. X* **2**, 041001 (2012).
 - [25] M. T. Reeves, T. P. Billam, B. P. Anderson, and A. S. Bradley, Inverse energy cascade in forced two-dimensional quantum turbulence, *Phys. Rev. Lett.* **110**, 104501 (2013).
 - [26] T. Simula, M. J. Davis, and K. Helmersson, Emergence of order from turbulence in an isolated planar superfluid, *Phys. Rev. Lett.* **113**, 165302 (2014).
 - [27] N. P. Müller and G. Krstulovic, Exploring the Equivalence between Two-Dimensional Classical and Quantum Turbulence through Velocity Circulation Statistics, *Physical Review Letters* **132**, 094002 (2024).
 - [28] S. P. Johnstone, A. J. Groszek, P. T. Starkey, C. J. Billington, T. P. Simula, and K. Helmersson, Evolution of large-scale flow from turbulence in a two-dimensional superfluid, *Science* **364**, 1267 (2019).
 - [29] G. Gauthier, M. T. Reeves, X. Yu, A. S. Bradley, M. A. Baker, T. A. Bell, H. Rubinsztein-Dunlop, M. J. Davis, and T. W. Neely, Giant vortex clusters in a two-dimensional quantum fluid, *Science* **364**, 1264 (2019).
 - [30] R. Fjørtoft, On the changes in the spectral distribution of kinetic energy for twodimensional, nondivergent flow, *Tellus* **5**, 225 (1953).
 - [31] Y. Zhu, B. Semisalov, G. Krstulovic, and S. Nazarenko, Direct and Inverse Cascades in Turbulent Bose-Einstein Condensates, *Physical Review Letters* **130**, 133001 (2023).
 - [32] H. K. Moffatt, The degree of knottedness of tangled vortex lines, *J. Fluid Mech.* **36**, 7 (1969).
 - [33] L. Biferale, S. Musacchio, and F. Toschi, Inverse energy cascade in three-dimensional isotropic turbulence, *Phys. Rev. Lett.* **108**, 164501 (2012).
 - [34] L. Biferale, S. Musacchio, and F. Toschi, Split energy-helicity cascades in three-dimensional homogeneous and isotropic turbulence, *J. Fluid Mech.* **730**, 309–327 (2013).
 - [35] G. Sahoo, A. Alexakis, and L. Biferale, Discontinuous transition from direct to inverse cascade in three-dimensional turbulence, *Phys. Rev. Lett.* **118**, 164501 (2017).
 - [36] F. Plunian, A. Teimurazov, R. Stepanov, and M. K. Verma, Inverse cascade of energy in helical turbulence, *J. Fluid Mech.* **895**, A13 (2020).
 - [37] J. Koplik and H. Levine, Vortex reconnection in superfluid helium, *Phys. Rev. Lett.* **71**, 1375 (1993).
 - [38] G. P. Bewley, M. S. Paoletti, K. R. Sreenivasan, and D. P. Lathrop, Characterization of reconnecting vortices in superfluid helium, *Proc. Natl. Acad. Sci. USA* **105**, 13707 (2008).
 - [39] C. Rorai, J. Skipper, R. Kerr, and K. Sreenivasan, Approach and separation of quantum vortices with balanced cores, *J. Fluid Mech.* **808**, 641 (2016).
 - [40] S. Serafini, L. Galantucci, E. Iseni, T. Bienaime, R. Bisset, C. F. Barenghi, F. Dalfovo, G. Lamporesi, and G. Ferrari, Vortex reconnections and rebounds in trapped atomic Bose-Einstein condensates, *Phys. Rev. X* **7**, 021031 (2017).
 - [41] L. Galantucci, A. W. Baggaley, N. G. Parker, and C. F. Barenghi, Crossover from interaction to driven regimes in quantum vortex reconnections, *Proc. Natl. Acad. Sci. USA* **116**, 12204 (2019).
 - [42] A. Villois, D. Proment, and G. Krstulovic, Universal and nonuniversal aspects of vortex reconnections in superfluids, *Physical Review Fluids* **2**, 044701 (2017).
 - [43] A. Villois, D. Proment, and G. Krstulovic, Irreversible dynamics of vortex reconnections in quantum fluids, *Phys. Rev. Lett.* **125**, 164501 (2020).
 - [44] L. Galantucci, A. W. Baggaley, C. F. Barenghi, and G. Krstulovic, A new self-consistent approach of quantum turbulence in superfluid helium, *Eur. Phys. J. Plus* **135**, 547 (2020).
 - [45] See supplementary materials.
 - [46] P. Z. Stasiak, Y. Xing, Y. Alihosseini, C. F. Barenghi, A. W. Baggaley, W. Guo, L. Galantucci, and G. Krstulovic, Experimental and theoretical evidence of universality in superfluid vortex reconnections, *arXiv* , 2411.08942 (2024).
 - [47] F. Waleffe, The nature of triad interactions in homogeneous turbulence, *Phys. Fluids A* **4**, 350 (1992).